cence microscopy. Microtubules with bound beads were observed with a simultaneous fluorescein isothiocyanate and Texas Red filter set (Chroma Technologies) and photographed on Ektachrome P1600 film (Kodak).
8. Polarity-marked microtubules were made as described [A. A. Hyman, *J. Cell Sci. Suppl.* **14**, 125 (1991)]. The marked, taxol-stabilized microtubules were purified away from soluble nucleotide and tubulin and incubated with beads as above.
9. Random microscope fields were selected for scoring. Microtubules that were shorter than the mean length were ignored, because these arise from shearing during pellet resuspension, as were microtubules that showed evidence of annealing (multiple bright segments). Of 200 microtubules scored, 190 had a bead bound only to the plus end, 6 only to the minus, and 4 to both ends.
10. L. G. Bergen, R. Kuriyama, G. G. Borisy, *J. Cell Biol.* **84**, 151 (1980). Tetrahymena axonemes were diluted in BRB80 and adsorbed to cover slips in perfusion chambers, which were then blocked with casein (10 mg/ml). Tubulin (24 μM) plus tetramethylrhodamine-labeled tubulin (6 μM) in BRB80 containing 1 mM GTP, 7 mM 2-mercaptoethanol, and 2% polyethylene glycol 8000 was perfused in and allowed to polymerize for 6 min at 37°C. The chambers were washed extensively with BRB80 containing 30 μM taxol; then 5 nM GTP-coated beads in the same buffer were perfused in and incubated for 1 hour. The chambers were washed and viewed by fluorescence microscopy. Initially the microtubules were not adherent to the substrate, and beads attached to plus ends were observed moving around attached to microtubule plus ends. For photography, we stuck down the microtubules by perfusing 100 nM kinesin into the chambers, followed by BRB80 containing 60% glycerol and 0.1% glutaraldehyde.
11. We scored 38 axonemes after photography. We observed 209 beads associated with plus ends and 6 with minus ends. The background sticking of beads to the cover slip near a microtubule end probably accounts for the minus-end binding.
12. Microtubule preparation and incubation with beads was as in (*7*) except that tetramethylrhodamine-labeled tubulin was omitted. The final microtubule pellet was diluted in BRB80 containing 30 μM taxol, adsorbed to freshly glow-discharged Formvar- and carbon-coated grids, negatively stained with 1% uranyl acetate, and imaged at 80 kV.
13. Taxol-stabilized microtubules were prepared free of soluble tubulin and GTP as in (*7*), and an aliquot was removed for determining number concentration by quantitative sedimentation onto cover slips. We incubated [α-^{32}P]GTP at various specific activities with microtubules in BRB80 containing 30 μM taxol for 3 min and then sedimented the microtubules through a glycerol-containing cushion to remove unbound nucleotide. The amount of bound nucleotide was determined by scintillation counting of the pellet, and the specific activity was corrected for the small amount of nucleotide present in the washed microtubule preparation and the low level of nonspecific binding. Under these conditions, the nucleotide was bound primarily to terminal E sites by two criteria: (i) Bound to each microtubule end were 10 ± 3 molecules of GTP. (ii) Up to 70% of the bound nucleotide in samples not subject to cross-linking was recovered as unhydrolyzed GTP. Nucleotide recovered from internal E sites was 100% hydrolyzed to GDP in control experiments. We cross-linked [α-^{32}P]GTP to tubulin by exposing the microtubule pellets to 260-nm light, as described for soluble tubulin (*13*). The α- and β-tubulin were resolved by electrophoresis in polyacrylamide gels containing sodium dodecyl sulfate contaminated with higher molecular weight alkyl chains. We confirmed the identity of the subunits (β-tubulin runs faster) by immunoblotting with monoclonal antibodies. Bands corresponding to α- and β-tubulin were excized and counted. Of the counts 99% were in the β-tubulin band and less than 1% in the α-tubulin band.
14. J. P. Nath, G. R. Eagle, R. H. Himes, *Biochemistry* **24**, 1555 (1985).
15. R. B. Vallee and H. S. Shpetner, *Annu. Rev. Biochem.* **59**, 909 (1990).
16. B. R. Oakley, *Trends Cell Biol.* **2**, 1 (1992).
17. Chemically cross-linked and sheared microtubules were reported to lack intrinsic GTPase activity [M. Caplow and J. Shanks, *J. Biol. Chem.* **265**, 8935 (1990)]. In preliminary experiments, we observed that [α-^{32}P]GTP bound to terminal E sites of taxol-stabilized microtubules (*13*) underwent much slower hydrolysis than nucleotide bound to internal E sites.
18. R. A. Walker, S. Inoue, E. D. Salmon, *J. Cell Biol.* **108**, 931 (1989).
19. I thank A. Hyman, M.-L. Wong, F. Malik, and P. Siebert for technical and intellectual help and K. Sawin and J. Howard for comments. This work was funded by NIH grant GM-39565 and a fellowship from the Packard Foundation.

22 March 1993; accepted 14 June 1993

Amyotrophic Lateral Sclerosis and Structural Defects in Cu,Zn Superoxide Dismutase

Han-Xiang Deng, Afif Hentati, John A. Tainer, Zafar Iqbal, Annarueber Cayabyab, Wu-Yen Hung, Elizabeth D. Getzoff, Ping Hu, Brian Herzfeldt, Raymond P. Roos, Carolyn Warner, Gang Deng, Edwin Soriano, Celestine Smyth, Hans E. Parge, Aftab Ahmed, Allen D. Roses, Robert A. Hallewell, Margaret A. Pericak-Vance, Teepu Siddique*

Single-site mutants in the Cu,Zn superoxide dismutase (SOD) gene (*SOD1*) occur in patients with the fatal neurodegenerative disorder familial amyotrophic lateral sclerosis (FALS). Complete screening of the *SOD1* coding region revealed that the mutation Ala^4 to Val in exon 1 was the most frequent one; mutations were identified in exons 2, 4, and 5 but not in the active site region formed by exon 3. The 2.4 Å crystal structure of human SOD, along with two other SOD structures, established that all 12 observed FALS mutant sites alter conserved interactions critical to the β-barrel fold and dimer contact, rather than catalysis. Red cells from heterozygotes had less than 50 percent normal SOD activity, consistent with a structurally defective SOD dimer. Thus, defective SOD is linked to motor neuron death and carries implications for understanding and possible treatment of FALS.

Amyotrophic lateral sclerosis (ALS), also called motor neuron disease, Charcot's disease, or Lou Gehrig's disease, is a progressive paralytic disorder that is usually fatal within 5 years of onset of symptoms (*1*). The paralysis is due to degeneration of large motor neurons of the brain and spinal cord; the underlying cause of the degeneration is not known (*2*). About 10% of ALS cases are familial. Familial ALS (FALS), clinically indistinguishable from sporadic ALS, is expressed as an age-dependent autosomal dominant trait (*3*, *4*). *SOD1*, the gene encoding the cytosolic antioxidant enzyme Cu,Zn superoxide dismutase (SOD), was studied as a FALS candidate because of (i) its proximity to a FALS locus mapped to chromosome 21q22.1 in a subset of FALS families (*5*–*7*), (ii) decreased SOD activity in cerebrospinal fluid of some ALS patients (*8*), (iii) the important function of SOD in free radical homeostasis (*9*), and (iv) the apparent role of free radicals in neurodegeneration (*10*). For 7 of the 11 previously reported FALS families (*5*, *6*) the probability of genetic linkage, based on heterogeneity analysis (*11*), to the region containing *SOD1* on chromosome 21 (*7*) was >90% (*6*). For three of the remaining families, linkage to this region was excluded; and for the fourth, results were inconclusive (*6*). Mutations in *SOD1* have been described in FALS families (*12*) but examined in only two (exons 2 and 4) of the five *SOD1* exons. The effects of the mutations on the enzyme's structure and function were not identified: they were hypothesized either to reduce or to increase the SOD activity. We now present the combined results from

H.-X. Deng, A. Hentati, A. Cayabyab, W.-Y. Hung, P. Hu, B. Herzfeldt, G. Deng, E. Soriano, C. Smyth, A. Ahmed, Department of Neurology, Northwestern University Medical School, 300 E. Superior Street, Chicago, IL 60611.
J. A. Tainer, E. D. Getzoff, H. E. Parge, Department of Molecular Biology, The Scripps Research Institute, La Jolla, CA 92037.
Z. Iqbal, Department of Neurology, Northwestern University Medical School, Chicago, and Northwestern University Institute of Neuroscience, Chicago, IL 60611.
R. P. Roos, Department of Neurology, University of Chicago, Chicago, IL 60637.
C. Warner, Department of Neurology, Dent Neurological Institute, Buffalo, NY 14209.
A. D. Roses and M. A. Pericak-Vance, Department of Medicine (Neurology), Duke University Medical Center, Durham, NC 27710.
R. A. Hallewell, Department of Biochemistry, Imperial College, London SW7 2AZ, U.K.
T. Siddique, Departments of Neurology and of Cell, Molecular, and Structural Biology, Northwestern University Medical School, Chicago, IL 60611, and Northwestern University Institute of Neuroscience.

*To whom requests for reprints should be addressed.

genetic screening of the entire *SOD1* coding region, SOD activity assays in human mutants, and x-ray crystallographic structure determination of human SOD, in order to characterize the FALS mutations, thus providing evidence for the specific structural basis of this disease.

Genomic DNA from members of FALS families and normal controls (*13*) was screened for mutations in *SOD1*. DNA amplified from the five *SOD1* exons (*14*) by polymerase chain reaction (PCR) was examined for single-stranded conformational polymorphism (SSCP) (*15*) by changes in DNA migration on nondenaturing polyacrylamide gels (Fig. 1). Such polymorphisms were heterozygous for the SOD1 mutations, and were detected in 17 of 49 FALS families tested, including 7 previously linked to the *SOD1* region of chromosome 21 (*5*, *6*), 2 with positive lod (logarithm of the odds of linkage) (*11*) scores for chromosome 21 markers (*5*, *6*), and 8 not tested for linkage. No sequence changes were found in exon 3 (*16*). Identical mobility changes representing SSCP in exon 1 appeared in eight families, whereas distinct SSCP patterns indicating different mutations were observed in each of exons 2, 4, and 5 (Fig. 1). No SSCPs were seen in DNA from the 75 normal controls, nor from the three FALS families (*6*) not linked to chromosome 21. Polymorphisms correlated appropriately with affected and at risk individuals segregating the affected haplotype, when DNA from all available members of the FALS families (Table 1) with the highest lod scores (individual multipoint lod scores of 2.32 for family 618C, and 3.46 for family 687C) was tested (*6*). Sequence analysis of DNA from affected individuals in all ten families with SSCPs in exons 1 and 5 revealed single base pair mutations (Fig. 2). The mutation (GCC → GTC) in exon 1 at position 4 removes a Hae III restriction site, thus producing the additional larger restriction fragment (49 bp) observed in these heterozygous mutants. Overall, 14 different single-site SOD mutants at 12 amino acid mutation sites have been identified (Table 1), accounting for the defects in 23 FALS families. The Ala^4 to Val mutation in exon 1 is the most frequent, occurring in eight different families.

We mapped the 12 mutation sites (Table 1 and Fig. 3) onto the human SOD crystallographic structure (Fig. 4) to define the effects of the FALS mutations on the protein structure and function. The wild-type human SOD structures, refined independently at 2.5 Å resolution in the $C222_1$, crystal form (*17*) and at 2.4 Å resolution in the $P6_3$ crystal form (*18*) were both used to assess the contributions of the side chains at these positions to the active site, the dimer interface, and the β barrel subunit fold, which exhibits Greek key topology [so named for a common design in Grecian art (*19*)]. We also examined comparable interactions within the crystallographic structures of bovine SOD, now refined at 1.8 Å resolution, and yeast SOD, now refined at 1.7 Å resolution (*18*). Overall, the structural results show that the 12 mutated side chains cluster near the two Greek key connections closing off the ends of the β barrel, in the dimer interface, and at the base of the active site loops (Figs. 3 and 4). These side chains, which are mostly sequence-conserved, are also structurally conserved in the wild-type SOD structures from different species, and appear to be critical for the structural integrity of the dimeric enzyme (Table 1). The FALS mutations do not change any active-site residues involved in the electrostatic recognition of the substrate (*20*), the ligation of the metal ions, or the formation of the active-site

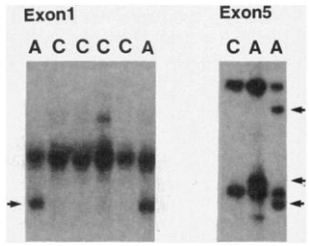

Fig. 1. Autoradiogram showing normal and variant (arrow) SSCP bands of DNA for exons 1 and 5 of SOD1, from patients with FALS (A) and control subjects (C). SSCP changes in the exon 1 panel are representative of affected individuals from families with a mutation in exon 1 (Table 1). DNA in lanes 2 and 3 of the exon 5 panel are from affected individuals in family 226C and 640C respectively. PCR primers used in the analysis were for exon 1: (i) TTC CGT TGC AGT CCT CGG AA and (ii) CGG CCT CGC AAC ACA AGC CT and for exon 5: (i) AGT GAT TAC TTG ACA GCC CA and (ii) TTC TAC AGC TAG CAG GAT AAC A. Primers for exons 2 and 4 have been reported in (*12*) as set b. PCR amplification, SSCP gel analysis [0.5 × Mutation Detection Enhancement (MDE; J. T. Baker), 5% glycerol gels], and autoradiography were performed essentially as described (*12*). Exon 1 and 5 PCR products were 158 bp and 216 bp, respectively. The Hae III restriction digests were performed as recommended (New England Biolab).

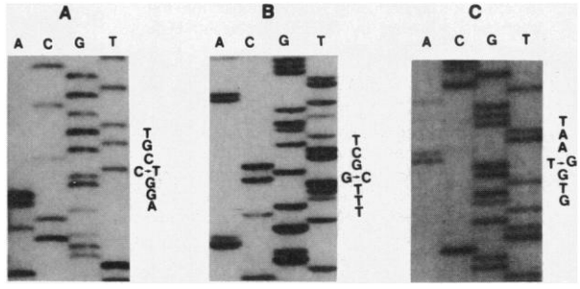

Fig. 2. Sequence analysis of DNA from affected individuals in FALS families listed in Table 1. (**A**) The only mutation identified in exon 1 (Table 1). The two exon 5 mutations (Table 1) are represented in (**B**) (family 640C) and (**C**) (family 226C). The vertically oriented sequence of seven bases to the right of each panel identify the mutation, the wild-type base is given to the left of the mutant, but is not represented in the autoradiograph. Primer sets in Fig. 1 were used to amplify exonic DNA essentially as previously described (*12*). The PCR products were purified and cloned into the plasmid PUC19 (*30*). Exon inserts in the plasmids were used to verify the normal and variant SSCP patterns expected and separately sequenced with Sequenase (USB). Both strands were sequenced in each instance.

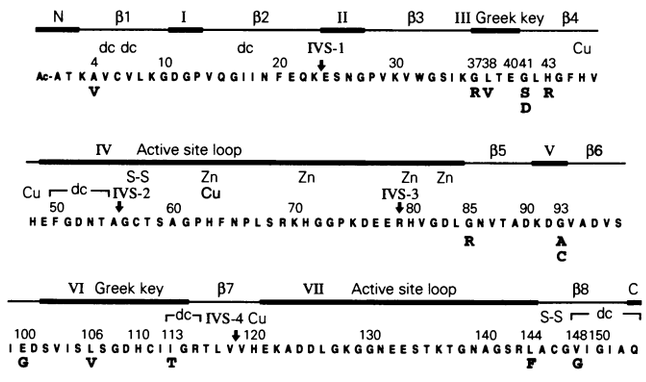

Fig. 3. Structural features and FALS associated mutations mapped to the amino acid sequence of human SOD, shown in single letter code. Ac indicates the NH_2-terminal acetyl group. The mutations at the 12 positions are shown in bold below the sequence. The mutation sites and every tenth residue are numbered above the sequence. The structural features shown at the top are the eight β strands of the Greek key β barrel, the seven connecting turns or loops (Roman numerals), NH_2-terminal (N) and COOH-terminal (C) sequences not present in β strands, and locations of four intervening sequences (IVS) showing the boundaries of the five exons. Residues that form a disulfide bridge (S-S), ligate the metals (Cu or Zn), or are involved in dimer contact (dc) are also shown above the sequence. Abbreviations for the amino acid residues are: A, Ala; C, Cys; D, Asp; E, Glu; F, Phe; G, Gly; H, His; I, Ile; K, Lys; L, Leu; M, Met; N, Asn; P, Pro; Q, Gln; R, Arg; S, Ser; T, Thr; V, Val; W, Trp; and Y, Tyr.

channel (Figs. 3 and 4). No mutations were found in exon 3, which encodes the Zn-binding loop of the active site (Fig. 3). Thus, these results point to a structurally defective and therefore less active enzyme, rather than to a completely inactive or a more active SOD in FALS.

On the basis of rigorous studies defining the structural and energetic effects of disrupting conserved hydrophobic packing interactions in proteins (*21*), six of the FALS mutations (Ala^4 to Val, Leu^{38} to Val, Leu^{106} to Val, Ile^{113} to Thr, Leu^{144} to Phe, Val^{148} to Gly) would be expected to destabilize the subunit fold or the dimer contact (Table 1 and Fig. 4). The most frequent FALS mutation (Ala^4 to Val) would disrupt both; the subunit fold, by collisions with the sequence-invariant Leu^{106} plug at one end of the β barrel (*19*), and the dimer interface, by shifts of the adjacent interface residue Val^5 (Fig. 4b). The His^{43} to Arg mutation removes a critical hydrogen bond, linking the first Greek key β barrel connection to the active site. The same mutation in yeast SOD (*18*) is accompanied by two additional compensatory sequence changes not found in this FALS mutant. The four FALS mutations that change sequence-conserved Gly residues would energetically destabilize the structurally conserved, left-handed, backbone conformation, favorable only to Gly. In contrast, the Glu^{100} to Gly mutation is expected to introduce potentially destabilizing flexibility at a β barrel connection next to the conserved salt bridge between Asp^{101} and Arg^{79}.

To investigate the influence of the structural defects in the FALS mutants on SOD activity, we measured the mean SOD activity in red cells (*22*) of 15 members of seven FALS families and found that the average mutant activity was less than half (41%) that of normal controls (Table 2). The 15 subjects were all heterozygous for *SOD1* mutations and represented six different mutations on exons 1, 2, 4, and 5, including the most frequent Ala^4 to Val mutation (Table 2). The mean SOD activity of individual mutation groups ranged from 36 to 47%. Activity gels on SOD from red cells confirmed that the His^{43} to Arg and the Glu^{100} to Gly mutants were expressed and had decreased activity (*22*), and therefore the disease is not simply the result of the absence of the mutant enzyme. The functional SOD enzyme is dimeric; thus, random association of wild-type and mutant subunits would result in 25% mutant homodimers, 25% wild-type homodimers, and 50% heterodimers. The apparent dominance of *SOD1* mutations in FALS may reflect the localization of these mutations to positions where both subunits of the dimer are affected (Fig. 4). This would be consistent with both the structural results and measured activities below 50%. SOD activity data from FALS mutants is in agreement with other biochemical studies of SOD mutants (*23*), and supports the structurally predicted destabilizing effects of these mutations, which can result in decreased Cu binding (*24*) and in reduced activity.

Although the general hypothesis that free radical mediated damage contributes to age-related neuropathology has been proposed (*10*), our results establish a specific molecular basis for free radical damage in a neurodegenerative illness resulting from a structurally defective SOD with reduced activity. Because of the scavenging of other free radicals by O_2 to form superoxide ($O_2^{\cdot -}$), SOD protects not only against direct damage by $O_2^{\cdot -}$ and damage from $O_2^{\cdot -}$-generated toxic hydroxyl radicals (from hydrogen peroxide) and peroxynitrite

Table 2. SOD activity in FALS mutants and controls.

Mutant	Subjects (*N*)	SOD activity* (mean ± SD)†	Mutation
Exon 1	4	1655 (± 487)	Ala^4 → Val
Exon 2	2	1499 (± 38)	His^{43} → Arg
Exon 4	3	1386 (± 327)	Gly^{85} → Arg
Exon 4	2	1256 (± 108)	Gly^{93} → Ala
Exon 4	2	1259 (± 410)	Glu^{100} → Gly
Exon 5	2	1252 (± 200)	Val^{148} → Gly
All mutants	15	1421 (± 333)†	Six different mutants
Controls	20	3506 (± 808)†	None

*In units per milligram of red cell protein. †Mean calculated from summation of individual sample readings. The SE of mutant mean = 86; 99% confidence limits 1165 to 1677 units; SE of control mean = 181, 99% confidence limits 2989 to 4023 units. The *t* test was used to calculate the difference between the two means, and the difference was statistically significant, $P < 0.0005$.

Table 1. FALS mutations in human SOD.

Amino acid change	Point mutation	Structural location‡	Structural role	FALS families
			Exon 1	
Ala^4 → Val	GCC → GTC	β strand	β barrel and dimer packing	587C, 618C, 649C, 687C, 827C, 1071C, 1109C, 9921C
			Exon 2	
Gly^{37} → Arg	GGA → AGA	Greek key connection	Conserved left-handed Gly	18†, 594C*
Leu^{38} → Val	CTG → GTG	Greek key connection	β barrel plug	11†
Gly^{41} → Ser	GGC → AGC	β strand	Conserved left-handed Gly	33†
Gly^{41} → Asp	GGC → GAC	β strand	Conserved left-handed Gly	36†
His^{43} → Arg	CAT → CGT	β strand	Hydrogen bonding	220C*
			Exon 4	
Gly^{85} → Arg	GGC → CGC	β strand	Conserved left-handed Gly	9967C*
Gly^{93} → Ala	GGT → GCT	Loop 5	Conserved left-handed Gly	3†§, 192C*§
Gly^{93} → Cys	GGT → TGT	Loop 5	Conserved left-handed Gly	57†
Glu^{100} → Gly	GAA → GGA	β strand	Stability for Greek key loop	684C*
Leu^{106} → Val	CTC → GTC	Greek key loop	Conserved β barrel plug	118†‖, 1209C‖
Ile^{113} → Thr	ATT → ACT	Greek key loop	Dimer interface packs self-symmetrically	130†, 385C*
			Exon 5	
Leu^{144} → Phe	TTG → TTC	β strand to loop connection	Packs with Leu^{38}	640C
Val^{148} → Gly	GTA → GGA	β strand	Dimer interface packs self-symmetrically	226C

*Mutation from Chicago (*12*). †Mutation from Boston (*12*). ‡See Figs. 3 and 4 for location. §Branches of the same family. ‖Branches of the same family.

anions (from the neurotransmitter nitric oxide), but also against damage from other intracellular free radicals generated metabolically or by environmental toxins (*9*, *25*). Apparently, the decreased SOD activity in FALS mutants described here is sufficient to protect against normal oxidative stress in most cells types, and may be partially compensated for by other human superoxide dismutases found in the mitochondria (MnSOD, *SOD2*) (*26*) and extracellular fluids (ECSOD, *SOD3*) (*27*). Although SOD immunoreactivity in large, long-lived, metabolically active neurons is increased compared to surrounding cells (*28*), it appears that SOD may not be readily inducible. Thus, *SOD1* mRNA levels remain unchanged after experimental axotomy, whereas MnSOD is upregulated (*29*). Motor neurons with FALS mutant SOD may be only marginally protected and may decompensate when challenged by increased free radical production in response to the metabolic demand of axonal sprouting due to age-related attrition of motor neurons (*3*) or other environmental challenge. Our results and free radical damage pathways suggest that both defects in protective enzymes (such as MnSOD, ECSOD, glutathione peroxidase, and catalase) and free radical generating toxins, need to be examined as candidates contributing to sporadic ALS, FALS not linked to chromosome 21, and other neurodegenerative diseases. In view of their central role in protection against free radicals, superoxide dismutases or similar agents may prove therapeutic for all forms of ALS that result from free radical damage.

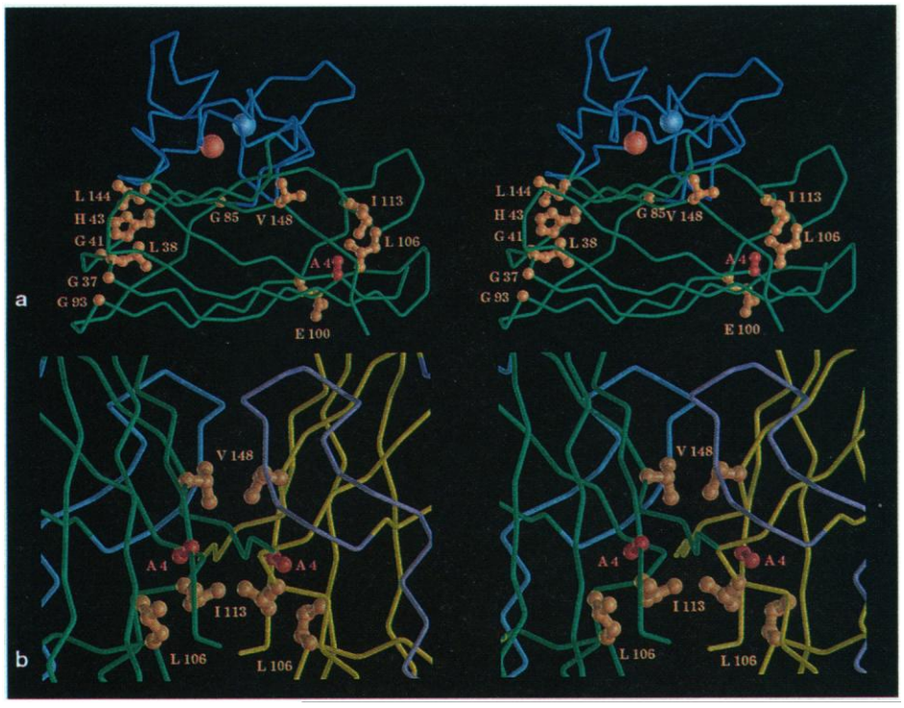

Fig. 4. Stereo pairs of the human SOD crystallographic structure showing the α-carbon backbone tubes and the side chains (stick and ball representation with 30% van der Waals radii) of residues mutated in FALS. These mutation sites involve changes to structurally conserved interactions in the human, bovine, and yeast SOD crystallographic structures. (**a**) In each subunit, viewed from the dimer interface direction, the side chains (orange) of mutated residues lie clustered at the two ends (left and right) of the β barrel (blue-green tubes) and at the base of the two major loops (blue tubes, top) forming the channel around the active site Cu (gold sphere) and Zn (blue sphere) ions. The most common FALS mutation site is Ala^4 (light red atoms and bonds), whose mutation to Val is expected to affect subunit and dimer stability and activity. Four of the mutations (at Gly^{37}, Gly^{41}, Gly^{85}, and Glu^{100}) should introduce charge changes, but their structural positions suggest that SOD activity will be affected primarily through destabilization, rather than through changes in the rate-limiting electrostatically facilitated diffusion of the substrate. For example, Gly^{85} to Arg disfavors a β bulge that helps to position the active-site metal ligands His^{46} and Asp^{83}. (**b**) Close-up of the twofold SOD dimer contact. The dimer interface includes β strand (blue-green versus yellow α-carbon traces distinguish the two subunits) and loop (blue versus purple α-carbon traces) interactions that also have an impact on the formation of the two active site channels (between loops on the outside surface of each subunit's β barrel). FALS mutations in residues forming twofold symmetric dimer interactions (Ile^{113} and Val^{148}) should most significantly destabilize the mutant homodimer and heterodimers. Changes to conserved hydrophobic packing interaction at one end of the β barrel adjacent to the dimer interface (Ala^4 and Leu^{106}) should directly destabilize the subunit fold by sterically disrupting the Ala close packing with Leu^{106}, the major hydrophobic plug for the end of the β barrel. Ala^4 and Leu^{106} changes are also expected to affect adjacent side chain and main chain dimer interface interactions. Although some hydrogen bonds from side chain to main chain are important to SOD folding and stability (*17*), the previous interpretation that changes to Leu^{106} and Ile^{113} might act by affecting these residues' main chain hydrogen bonding (*12*) seems less probable from the SOD structures than the direct disruption of their specific hydrophobic packing interactions proposed here.

REFERENCES AND NOTES

1. D. B. Williams and J. A. Windebank, in *Peripheral Neuropathy*, P. J. Dyck, P. K. Thomas, J. W. Griffin, P. A. Low, J. F. Poduslo, Eds. (Saunders, Philadelphia, ed. 3, 1993), pp. 1028–1050.
2. A. Hirano and M. Iwata, in *Amyotrophic Lateral Sclerosis*, T. Tsubaki and Y. Toyokuro, Eds. (University Park Press, Baltimore, 1979), pp. 107–133; R. Tandan and W. G. Bradley, *Ann. Neurol.* **36**, 271; *ibid.*, p. 419.
3. D. W. Mulder, L. T. Kurland, K. P. Offord, C. M. Beard, *Neurology* **36**, 511 (1986).
4. T. Siddique *et al.*, *ibid.* **39**, 919 (1989).
5. T. Siddique *et al.*, *N. Engl. J. Med.* **324**, 1381 (1991).
6. T. Siddique *et al.*, *Int. J. Neurol.*, in press; T. Siddique *et al.*, unpublished results.
7. S. E. Antonarakis, *Genomics* **14**, 1126 (1992).
8. F. Bracco, M. Scarpa, A. Rigo, L. Battistin, *Proc. Soc. Exp. Biol. Med.* **196**, 36 (1991).
9. I. Fridovich, *Arch. Biochem. Biophys.* **247**, 1 (1986); B. Halliwell and J. M. C. Gutteridge, *Free Radicals in Biology and Medicine* (Clarendon Press, Oxford, ed. 2, 1989).
10. B. Halliwell and J. M. C. Gutteridge, *Trends Neurosci.* **8**, 22 (1985); C. W. Olanow, *Neurology* **40** (suppl. 3), 32 (1990).
11. J. Ott, *Analysis of Human Genetic Linkage* (John Hopkins Univ. Press, Baltimore, ed. 2, 1991), pp. 203–216.
12. D. R. Rosen *et al.*, *Nature* **362**, 59 (1993).
13. Informed consent was obtained from participating subjects before collection of blood samples for DNA analysis and SOD assay. DNA was extracted as described (*5*).
14. R. A. Hallewell, J. P. Puma, G. T. Mullenbach, R. C. Najarian, in *Superoxide and Superoxide Dismutase in Chemistry, Biology and Medicine*, G. Rotillo, Ed. (Elsevier, Amsterdam, 1986), pp. 249–256.
15. M. Orita, Y. Suzuki, T. Sekiya, K. Hayashi, *Genomics* **5**, 874 (1989).
16. For the SSCP noted with exon 3 primers (T. Siddique *et al.*, unpublished results), the amplified DNA was sequenced and found to have a point mutation (GAT → GCT) at the 34th nucleotide in the intron, 3′ to the end of exon 3. This mutation created an Hha I site and gave rise to two additional smaller DNA fragments in heterozygotes. This rare polymorphism was also seen in 4% of normal controls.
17. H. E. Parge, R. A. Hallewell, J. A. Tainer, *Proc. Natl. Acad. Sci. U.S.A.* **89**, 6109 (1992).
18. To evaluate the structural function and interactions of the wild-type residues that are mutated in FALS, we used the results from the structural determination and refinement of two distinct crystal forms of wild-type human SOD1. (i) A new space group $P6_3$ crystal form, $a = b = 113.5$ Å, $c = 71.5$ Å, crystallized from PEG 4000, with one dimer per asymmetric unit, refined to 2.4 Å resolution with an R value of 22.4% without solvent, and (ii) a space group $C222_1$ crystal form, $a = 205.2$, $b = 167.0$, $c = 145.5$ Å, crystallized from ammonium sulfate [H. E. Parge *et al.*, *J. Biol. Chem.* **261**, 16215 (1986)], with five dimers per asymmetric unit, refined to 2.5 Å resolution with an

R value of 21% with solvent (*17*). For the wild-type human SOD $P6_3$ crystal form, we collected 140,309 observations of 17,554 unique reflections representing 89.8% of the diffraction data to 2.4 Å resolution. The orientation was determined with Crowther's rotation function as implemented in MERLOT [P. M. D. Fitzgerald, *J. Appl. Crystallogr.* **21**, 273 (1988)] with the use of the "humanized" bovine enzyme as the search probe, and the position was found by means of an *R* factor search in XPLOR [A. T. Brünger, J. Kuriyan, M. Karplus, *Science* **235**, 458 (1987)]. The initial *R* factor after rigid group refinement was 43%, and the current *R* factor after conventional refinement with PROLSQ and one round of simulated annealing with XPLOR was 22.4% for the data between 5 and 2.4 Å resolution with overall deviations from ideal geometry of 0.04 Å for bond distances and 3.5° for bond angles. To evaluate the role of these residue interactions identified in the two human SOD structures in the stability of the SOD fold and its dimer assembly, the residue interactions at positions mutated in FALS patients were checked for conservation within the structures of bovine SOD refined to 1.8 Å resolution with an *R* value of 17% (S. Redford, D. McRee, J. Tainer, E. Getzoff, unpublished results) and yeast SOD refined to 1.7 Å resolution with an *R* value of 18% (H. Parge, J. Tsang, K. Slater, J. Valentine, J. Tainer, unpublished results). Buried surface areas, packing interactions, and residue pair contacts were quantitated as described (*26*).

19. E. D. Getzoff, J. A. Tainer, M. M. Stempien, G. I. Bell, R. A. Hallewell, *Proteins: Struct. Func. Genet.* **5**, 322 (1989).
20. E. D. Getzoff *et al.*, *Nature* **358**, 347 (1992).
21. A. E. Eriksson *et al.*, *Science* **255**, 178 (1992); N. S. Scrutton, M. P. Deonarain, A. Berry, R. N. Perham, *ibid.* **258**, 1140 (1992); D. Mendel *et al.*, *ibid.* **256**, 1798 (1992); W. S. Sandberg and T. C. Terwilliger, *ibid.* **245**, 54 (1989); D. E. McRee *et al.*, *J. Biol. Chem.* **265**, 14234 (1990).
22. The SOD activity was measured in partially purified enzyme protein preparation. The red cells, washed three times with phosphate-buffered saline in cold, were lysed with 50 mM potassium-phosphate buffer, pH 7.4, and the lysate was treated with 0.4 volume of an ethanol:chloroform (25:15, v/v) mixture to remove hemoglobin as described [J. M. McCord and I. Fridovich, *J. Biol. Chem.* **244**, 6049 (1969)]. The hemoglobin-free supernatant was mixed with potassium hydrogen phosphate (K_2HPO_4, final concentration of 300 mg/ml), and allowed to stand at room temperature. The clear supernatant obtained after centrifugation (5000*g* for 15 min) was cooled and treated with two volumes of acetone, and precipitated proteins were dissolved in 50 mM potassium-phosphate buffer, pH 7.8, reprecipitated with acetone, and dissolved in the buffer. Enzyme activity was assayed at 37°C as described [D. R. Spitz and L. W. Oberley, *Anal. Biochem.* **179**, 8 (1989)] by monitoring the reduction in blue formazan formation (L. W. Oberley and D. R. Spitz, in *CRC Handbook of Methods for Oxygen Radical Research*, R. Greenwald, Ed. (CRC Press, Boca Raton, FL, 1985), pp. 217–220). The assay mixture (1 ml) contained 50 mM potassium-phosphate buffer, pH 7.8, 56 μM nitroblue tetrazolium, 100 μM xanthine, 50 μM bathocuproine disulfonic acid (BCDA), 1 mM diethylene triamine pentaacetic acid, 130 μg of BSA, 1 unit of catalase, SOD-containing protein preparations at several concentrations, and an appropriate amount of xanthine oxidase to give ΔA/min of 0.025 to 0.035 at 560 nm. A unit of enzyme activity is defined as the amount of protein required for half-maximal inhibition of formazan formation. Assays were done in duplicate. Activity gels of red cell lysates were run as described [C. Beauchamp and I. Fridovich, *Anal. Biochem.* **44**, 276 (1971)]; Z. Iqbal *et al.*, unpublished data.
23. R. A. Hallewell *et al.*, *Nucleic Acids Res.* **13**, 2017 (1985); R. A. Hallewell, E. D. Getzoff, J. A. Tainer, unpublished data.
24. For SOD: R. A. Hallewell, D. Cabelli, E. D. Getzoff, unpublished data; for other Cu enzymes: M. Nishiyama *et al.*, *Protein Eng.* **5**, 177 (1992).
25. J. S. Beckman, T. W. Beckman, J. Chen, P. A. Marshall, B. A. Freeman, *Proc. Natl. Acad. Sci. U.S.A.* **87**, 1620 (1990); C. F. Kuo, T. Mashino, I. Fridovich, *J. Biol. Chem.* **262**, 4724 (1987); W. H. Koppenol, J. J. Moreno, W. A. Pryor, H. Ischiropoulos, J. S. Beckman, *Chem. Res. Toxicol.* **5**, 834 (1992); C. C. Winterbourn, *Free Rad. Biol. Med.* **14**, 85 (1993); J. O. McNamara and I. Fridovich, *Nature* **362**, 20 (1993); S. Przedborski *et al.*, *J. Neurosci.* **12** (5), 1658 (1992).
26. Y. S. Ho, A. J. Howard, J. D. Crapo, *FEBS Lett.* **229**, 256 (1988); G. E. O. Borgstahl *et al.*, *Cell* **71**, 107 (1992).
27. K. Hjalmarsson, S. L. Marklund, Å. Engström, T. Edlund, *Proc. Natl. Acad. Sci. U.S.A.* **84**, 6340 (1987).
28. I. Ceballos *et al.*, *Free Rad. Res. Commun.* **12–13**, 571 (1991); T. Siddique *et al.*, unpublished data.
29. T. Yoneda, S. Inagaki, Y. Hayashi, T. Nomura, H. Takagi, *Brain Res.* **582**, 342 (1992).
30. J. Sambrook, E. F. Fritsch, T. Maniatis, *Molecular Cloning* (Cold Spring Harbor Laboratory Press, Cold Spring Harbor, NY, ed. 2, 1989), pp. 1.13–1.14.
31. This paper is dedicated to the memory of Forbes H. Norris, Jr., and patients we lost to ALS. We thank our teachers, A. Ahmed, S. D. Cook, P. Tsairis, and W. K. Engel, who taught us the care of patients with ALS and who encouraged this research; N. Siddique, J. Braun, J. Sacks, P. Casey, J. Richman, H. Mitsumoto, and R. Tandan for help in obtaining blood samples and pedigree information; M. E. Pique for help with computer graphics; and J. Rimmler and P. Pate for help with linkage analysis. Supported by the Les Turner ALS Foundation (T.S.), the NINDS (T.S., M.A.P.-V., H.-X.D., R.P.R.), the NIGMS (J.A.T., R.A.H., E.D.G.) and CRC grant (A.D.R., T.S., M.A.P-V.), the ALS Association (T.S., G.D.), the Gisela Fund for ALS research (T.S.), the Muriel Heller Fellowship Fund for ALS Research (W.-Y.H.), the Muscular Dystrophy Association (T.S., M.A.P.-V., A.H.), H.C. and F. Wenske Foundation (T.S.), the Searle Family Fund for Neurological Disorders (T.S.), the Vena E. Schaaf ALS Research Fund (T.S.), and Atropos Genetic Engineering, Inc. (R.A.H.). Atomic coordinates have been deposited in the Brookhaven Protein Databank code 1SPD.

23 March 1993; accepted 19 July 1993

An Essential Role for Protein Phosphatases in Hippocampal Long-Term Depression

Rosel M. Mulkey, Caroline E. Herron, Robert C. Malenka*

The effectiveness of long-term potentiation (LTP) as a mechanism for information storage would be severely limited if processes that decrease synaptic strength did not also exist. In area CA1 of the rat hippocampus, prolonged periods of low-frequency afferent stimulation elicit a long-term depression (LTD) that is specific to the stimulated input. The induction of LTD was blocked by the extracellular application of okadaic acid or calyculin A, two inhibitors of protein phosphatases 1 and 2A. The loading of CA1 cells with microcystin LR, a membrane-impermeable protein phosphatase inhibitor, or calmodulin antagonists also blocked or attenuated LTD. The application of calyculin A after the induction of LTD reversed the synaptic depression, suggesting that phosphatase activity is required for the maintenance of LTD. These findings indicate that the synaptic activation of protein phosphatases plays an important role in the regulation of synaptic transmission.

Activity-dependent long-term changes in synaptic efficacy are of fundamental importance for the development of neural circuits and for information storage in the nervous system. Long-term potentiation in area CA1 of the hippocampus has been an intensively studied form of activity-dependent synaptic plasticity primarily because it can be elicited reliably in vitro in isolated slices of the hippocampus. Consequently, some of the biochemical steps responsible for its induction and maintenance are well characterized (*1*).

Several different forms of LTD in the hippocampus have been observed (*2*), although the underlying biochemical mechanisms are not known. Recently a form of LTD that, like LTP, is restricted to activated synapses has been described (*3*, *4*). This homosynaptic LTD requires activation of postsynaptic *N*-methyl-D-aspartate (NMDA) receptors (*3*, *4*) and a change in the postsynaptic Ca^{2+} concentration (*4*). We have examined biochemical processes underlying this form of LTD and find that LTD requires serine-threonine protein phosphatase activity.

Synaptic transmission between Schaffer collateral-commissural afferent fibers and CA1 pyramidal cells in rat hippocampal slices was studied with standard extracellular and whole-cell recording techniques (*5*). After LTD was saturated with repetitive periods (2 to 6 min) of 1-Hz stimulation (*4*), LTP-inducing high-frequency tetanuses (100 Hz, 1 s) increased synaptic strength beyond the original baseline value (Fig. 1). If the induction of LTP had not caused a reversal of the processes responsible for LTD, it would not have been possible to re-elicit LTD. Instead, additional episodes of 1-Hz stimulation reduced synaptic strength to its original minimal saturated level (10 of 12 experiments) (Fig. 1). Consistent with this finding, previous work has

Departments of Psychiatry and Physiology, University of California, San Francisco, CA 94143–0984.

*To whom correspondence should be addressed.